

## Electron-paramagnetic-resonance observation of gallium vacancy in electron-irradiated *p*-type GaAs

Y. Q. Jia and H. J. von Bardeleben

*Groupe de Physique des Solides de l'Université Paris 7, Tour 23, 2 place Jussieu, 75251 Paris CEDEX 05, France*

D. Stievenard and C. Delerue

*Institut Supérieur d'Electronique du Nord, Laboratoire de Physique des Solides, 41 Boulevard Vauban, 59046 Lille CEDEX, France*

(Received 20 June 1991)

We report an observation by electron paramagnetic resonance (EPR) of the gallium vacancy defect in GaAs. The defect is observed after electron irradiation of *p*-type GaAs. The gallium vacancy defect shows trigonal symmetry; its spin-Hamiltonian parameters are determined as  $S = \frac{1}{2}$ ,  $g_{\parallel[111]} = 1.98 \pm 0.02$ ,  $g_{\perp[111]} = 2.08 \pm 0.01$ ,  $A_{\parallel[111]} = (280 \pm 20) \times 10^{-4} \text{ cm}^{-1}$ , and  $A_{\perp[111]} = (130 \pm 10) \times 10^{-4} \text{ cm}^{-1}$ . A tight-binding Green's function calculation confirms the defect model and identifies its charge state as  $2^-$ . The gallium vacancy is unstable at room temperature, the thermal annealing parameters being Fermi-level dependent.

### I. INTRODUCTION

Native defects in as-grown as well as irradiated GaAs materials remain a subject of active research.<sup>1</sup> A number of experimental results have been published on the observation of defects in the arsenic sublattice. Deep-level-transient-spectroscopy (DLTS) studies on electron-irradiated *n*- and *p*-type samples have established a series of electron traps (labeled *E1–E5*) and hole traps (labeled *H0–H5*). Most of these traps (except *H2–H5*) have been attributed to defects in the As sublattice, i.e., As-vacancy–As-interstitial Frenkel pairs in various configurations.<sup>2,3</sup> Positron annihilation (PA) results<sup>4</sup> provided further evidence of the existence of the As vacancy in irradiated samples. Electron-paramagnetic-resonance (EPR) studies have revealed three dominant defects in electron-irradiated *n*-type GaAs, one of which is correlated to the As antisite and the other two to defects associated with the As vacancy.<sup>5,6</sup> Less information is known about the Ga vacancy, and in particular no EPR study, to our knowledge, has been reported before.

Although the Ga vacancy has been evoked in recent studies, no direct information on its microscopic structure could be obtained. In particular it has often been considered that the Ga vacancy plays an important role in the free-carrier compensation<sup>7</sup> and the impurity diffusion.<sup>8</sup> It was predicted<sup>9</sup> from theoretical calculations that the Ga vacancy would be a stable defect in all neutral or negative charge states while a structural change would occur when it was positively charged. Experimental studies of native defects in GaAs have made use of high-energy electron irradiation which produces primary defects in both sublattices.<sup>10</sup> However, DLTS studies have not evidenced any Ga-vacancy-related deep levels in electron-irradiated GaAs.<sup>2,3</sup> Recent positron lifetime results, on the contrary, revealed a negatively charged vacancy in electron-irradiated *p*-type GaAs which has been attributed to the Ga-vacancy defect.<sup>11</sup> In

this work we report an EPR spectrum in 1-MeV electron-irradiated *p*-type GaAs and present strong evidence for the identification of this spectrum with the  $2^-$  charge state of the Ga vacancy.

### II. EPR RESULTS

*p*-type ( $[\text{Zn}] = 4.6 \times 10^{16} \text{ cm}^{-3}$ ) GaAs samples have been irradiated with 1-MeV electrons at room temperature. The irradiation was performed with a Van de Graaff accelerator. Water cooling and small electron flux ( $0.7 \mu\text{A}/\text{cm}^{-2}$ ) have been used to avoid the heating of the sample above  $T = 30^\circ\text{C}$  during irradiation. Electron doses range from  $2 \times 10^{16}$  to  $1 \times 10^{18} \text{ cm}^{-2}$ . After irradiation, all samples have been kept in liquid nitrogen before the EPR measurements. The EPR measurements were carried out at 4 K with an X-band spectrometer working at 9.37 GHz. For electron doses higher than  $2 \times 10^{17} \text{ cm}^{-2}$  all samples showed in thermal equilibrium a superposition of at least two different EPR spectra. One of them is the  $\text{As}_{\text{Ga}}$  defect.<sup>12</sup> After subtracting this antisite spectrum, we obtain a spectrum (see Fig. 1) whose angular variation is shown in Fig. 2(a). Its spin concentration increases linearly with electron dose as is shown in Fig. 3, from which we estimate the production rate to be  $0.03 \text{ cm}^{-1}$ .

The orientation dependence of the EPR spectrum implies a trigonal symmetry of the defect. (Further analysis led us to recognize that the central hyperfine splitting comes from one atom whose nuclear spin should be  $\frac{3}{2}$ .) The experimental spectrum has been simulated with the following spin Hamiltonian:

$$\hat{H} = \mu_B \mathbf{B} \cdot \vec{g} \cdot \mathbf{S} + \mathbf{S} \cdot \vec{A} \cdot \mathbf{I}, \quad (1)$$

with  $S = \frac{1}{2}$ ,  $I = \frac{3}{2}$ . Since both As and Ga atoms have  $I = \frac{3}{2}$  nuclear spin, we have considered two cases: first, a central hyperfine interaction with one As ( $^{75}\text{As}$ :  $I = \frac{3}{2}$ ,

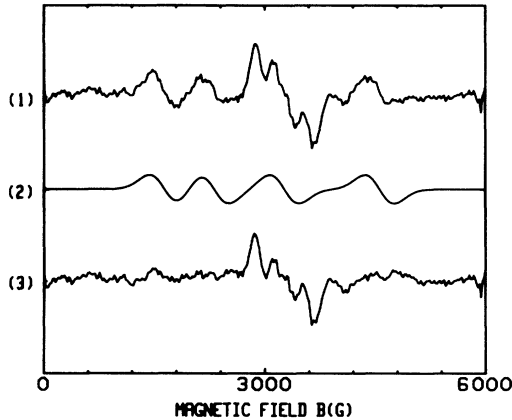


FIG. 1. (1) EPR signal at 4-K thermal equilibrium of Zn-doped GaAs sample after a dose of  $1 \times 10^{18} \text{ cm}^{-2}$ , 1-MeV electron.  $\mathbf{B}_{\parallel[001]}$ ,  $h\nu=9.37 \text{ GHz}$ , and the microwave power  $P=2 \text{ mW}$ . (2) Simulation spectrum for As antisite. (3) After subtraction the Ga vacancy spectrum becomes the dominant signal.

100%); and second, a central hyperfine interaction with one Ga ( $^{71}\text{Ga}$ :  $I=\frac{3}{2}$ , 40%;  $^{69}\text{Ga}$ :  $I=\frac{3}{2}$ , 60% abundance). It has been found that for both cases, a good spectrum simulation can be obtained with the following  $g$  values:

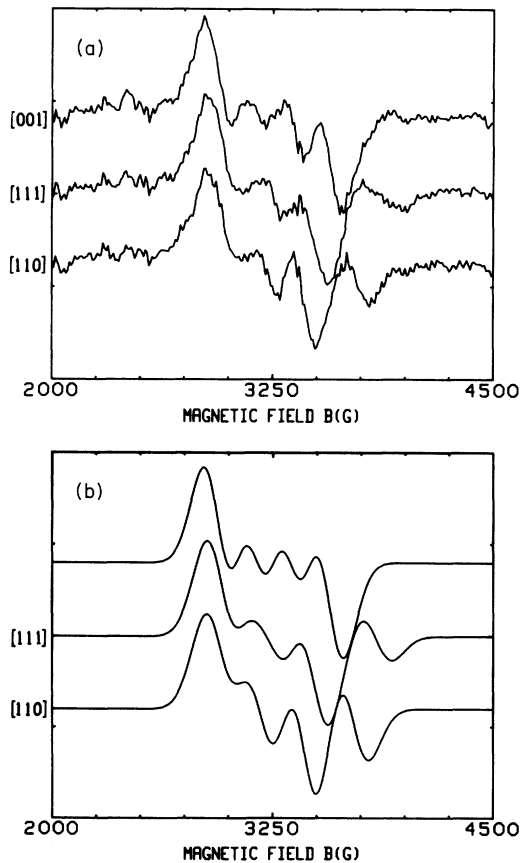


FIG. 2. (a) Orientation dependence of Ga-vacancy spectrum. Taken for  $\mathbf{B}_{\parallel[001]}$ ,  $[111]$ , and  $[110]$ . (b) Simulation spectrum for the above three orientations. Parameters are given in the text.

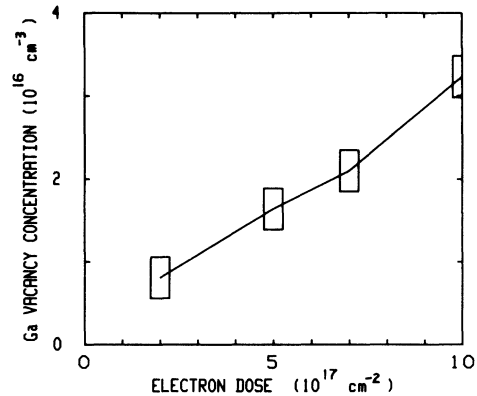


FIG. 3. The Ga-vacancy concentration vs electron dose.

$$g_{\parallel[111]}=1.98\pm 0.02 \quad \text{and} \quad g_{\perp[111]}=2.08\pm 0.01 .$$

As for the hyperfine tensor, we found the axial direction of the  $A$  tensor should be the same as that of the  $g$  tensor. In the first case, hyperfine interaction with one As, the experimental spectrum is well fitted with

$$A_{\parallel[111]}=(280\pm 20)\times 10^{-4} \text{ cm}^{-1}$$

and

$$A_{\perp[111]}=(130\pm 10)\times 10^{-4} \text{ cm}^{-1} .$$

When considering two isotopes such as  $^{69}\text{Ga}$  and  $^{71}\text{Ga}$ , we note that the hyperfine values corresponding to  $^{69}\text{Ga}$  and  $^{71}\text{Ga}$  should be different (with a ratio of  $^{69}A : ^{71}A = ^{69}g_N : ^{71}g_N = 1.344 : 1.708$ ). We have

$$^{71}A_{\parallel[111]}=(300\pm 20)\times 10^{-4} \text{ cm}^{-1} ,$$

$$^{71}A_{\perp[111]}=(150\pm 10)\times 10^{-4} \text{ cm}^{-1}$$

for the two-isotope simulation. The individual linewidth is found to be  $190\pm 10 \text{ G}$ . The above hyperfine splitting values are, however, not large enough (relative to the individual linewidth) to allow a clear distinction between the two cases, contrary to the case of the Ga interstitial in  $\text{Al}_{1-x}\text{Ga}_x\text{As}$ , where the larger hyperfine splitting ( $640\times 10^{-4} \text{ cm}^{-1}$  for  $^{71}\text{Ga}$ ) made it easy to identify the Ga origin.<sup>13</sup> Nonetheless, we found that the one isotope simulation gives a better fit in aspect of the fine structure. The simulated spectrum for the one-isotope case is shown in Fig. 2(b); its angular dependence for a rotation of the magnetic field in the (110) plane is shown in Fig. 4. A comparison of the above two sets of hyperfine data with the free-atom values<sup>14</sup> indicates that 49% of the electron wave function would be localized on the As atom (if the  $A$  tensor is due to an As atom) and 62% of that on the Ga atom (if the  $A$  tensor is due to a Ga atom). Both these values of electron localization are consistent with the identification of the spectrum as due to a dangling-bond-like defect. Several trigonal symmetric EPR spectra in GaAs have been reported before.<sup>15-17</sup> They are different from our spectrum by both the  $g$  and  $A$  values.

Strong arguments are available to identify our spectrum as the Ga vacancy. First, this spectrum is detect-

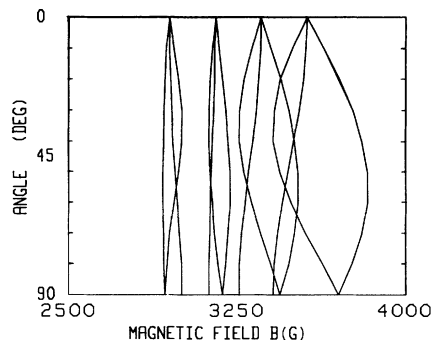


FIG. 4. Calculated angular dependence of resonance fields with  $B$  in a (011) plane. The angle is between the field direction and the [100] lattice axis. The microwave frequency is 9.37 GHz.

able in the dark after an electron dose as low as  $1 \times 10^{17} \text{ cm}^{-2}$ , while the As antisite spectrum cannot be detected at the same time (the As antisite spectrum appears under optical excitation). Therefore, we learn that the paramagnetic level of the new defect should be lower than the  $+2$  level of the  $\text{As}_{\text{Ga}}$  antisite, i.e., lower than  $E_v + 0.52 \text{ eV}$ .<sup>1</sup> It has been well understood from theoretical calculations by various authors that the Ga vacancy tends to produce deep levels in the lower midgap while the As vacancy levels are situated in the upper midgap (see next section). Second, we have found that our spectrum partially anneals at room temperature. For example, after the first measurement, sample no. 7 (dose =  $1 \times 10^{18} \text{ cm}^{-2}$ ) has been kept at 77 K except for being exposed in air for about two days. When we remeasured this sample under the same conditions as the first measurement, we found the intensity of the new spectrum has been reduced by a factor of nearly 2. We show the partial annealing behavior in Fig. 5. This weak thermal stability is quite different from that of As-vacancy-related defects which anneal in two stages (at  $\sim 500$  and 700 K) as determined from DLTS studies.<sup>2,3</sup> Third, the isotropic part of the spin-electron wave function, i.e., the localization part on the  $s$  orbital of the dangling bond can be determined from the experimental hyperfine values. We find that 3.7%  $s$

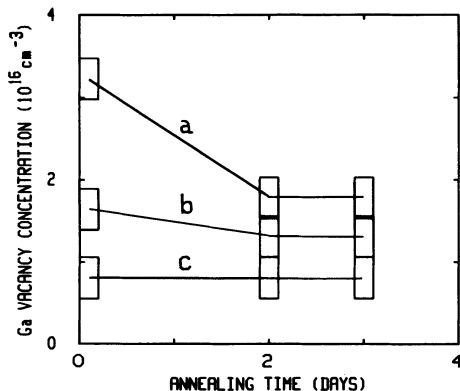


FIG. 5. Partial annealing of Ga vacancy at room temperature. Three samples denoted  $a$ ,  $b$ , and  $c$  in the figure have been irradiated with doses of  $1.0 \times 10^{18}$ ,  $5 \times 10^{17}$ , and  $2 \times 10^{17} \text{ cm}^{-2}$ , respectively.

density would be found for an As dangling bond and 3.9% on a Ga dangling bond. Thus whatever the dangling-bond atom is, the  $s$  density is always found to be very small. This small  $s$  density can only be explained for the Ga vacancy. From our theoretical calculations (see the next section) a trigonal distorted Ga vacancy results in a small  $s$  density (7%) of electron localization on the dangling-bond atom while a trigonal distorted As vacancy gives a large  $s$  density (17%).

### III. THEORETICAL CALCULATION

To explain the above EPR results, particularly the hyperfine data, we have carried out a tight-binding Green's-function (TBGF) calculation<sup>18</sup> for various intrinsic defects. A more detailed description of the calculation can be found in another paper.<sup>19</sup> We have found that among the simple intrinsic point defects in GaAs, the As interstitial does not introduce any deep levels in the lower midgap and its electron localization on the As interstitial is incompatible with our EPR hyperfine data; the same is valid for the electron localization on the Ga interstitial. Thus we concentrate in the following on the Ga-vacancy and As-vacancy cases.

First, we deal with the ideal nondistorted vacancies, i.e., of  $T_d$  symmetry. We find in agreement with previous results<sup>20-22</sup> that both the Ga vacancy and As vacancy introduce  $t_2$  deep states in the gap with the level position depending on the charge state of the vacancy. For the neutral Ga vacancy, the highest occupied  $t_2$  level is at  $E_v + 0.13 \text{ eV}$  with three electrons on the  $t_2$  level, and shifts to  $E_v + 0.57 \text{ eV}$  with six electrons on the  $t_2$  level. When the occupation number is smaller than 3, the  $t_2$  level becomes resonant with the valence band. As for the As vacancy, the  $t_2$  level is located between  $E_v + 0.83 \text{ eV}$  with one electron on the  $t_2$  level and  $E_v + 1.26 \text{ eV}$  with four electrons on the  $t_2$  level. Hence, the Ga vacancy tends to introduce a  $t_2$  level in the lower midgap while for the As vacancy they are in the upper midgap.

Lattice relaxation will modify these results as follows: in fact, at the first occupation of an electron onto the  $t_2$  level, the vacancy should undergo a distortion. In our case, we observed a trigonally distorted defect, which is of the same symmetry as that of the Zn vacancy in ZnSe.<sup>23</sup> Under a trigonal distortion the  $t_2$  level splits into a nondegenerate  $a_1$  level and a double degenerate  $e$  level. We know that the EPR-detected electron should be occupying the  $a_1$  level, otherwise the single occupation onto the  $e$  level would induce further distortion to reduce the symmetry from  $C_{3v}$  to a lower symmetry.

To have an unpaired electron level in the gap, the  $t_2$  level of the Ga vacancy should be occupied by three or five electrons (one electron occupation leads to the  $t_2$  level into the valence band). However, as has been discussed in Ref. 24, a population of three electrons would lead to a mixed distortion and would not result in the observed  $C_{3v}$  symmetry. Therefore, only the five-electron occupation on the  $t_2$  level is compatible with our EPR results. In the same way we find for the As vacancy that only a one-electron occupation on the  $t_2$  level will give rise to an

unpaired electron level in the gap. As has been indicated in Ref. 24, in the case of one-electron occupation on the  $t_2$  level, after distortion the  $a_1$  level is lower than the  $e$  level, while in the case of five-electron occupation, the  $e$  level (filled with four electrons) is lower than the  $a_1$  level (filled with one electron). Hence, the unpaired electron is always in the  $a_1$  state. With five electrons filling the  $t_2$  level, the Ga vacancy should be doubly negatively charged, while with one electron filling the  $t_2$  level, the As vacancy should be in neutral charge state. Therefore, we have two EPR-active vacancy defects:  $V_{\text{Ga}}^{2-}$  and  $V_{\text{As}}^0$ .

In a simple perturbation theory, the  $a_1$  state, issued from the  $t_2$  state, can be written as

$$\frac{1}{\sqrt{3}}(t_{2x} + t_{2y} + t_{2z}), \quad (2)$$

where  $t_{2x,y,z}$  represents the three degenerate states of the original  $t_2$  triplet. Then, the  $a_1$ -state wave function can be obtained after the calculation of the  $t_2$ -state wave function. For the Ga vacancy, we first calculate the  $t_2$ -state wave function of  $V_{\text{Ga}}^{2-}$  level at  $E_v + 0.39$  eV, and then get the  $a_1$ -state wave function by use of Eq. (2). We find the electron is primarily centered onto the one nearest-neighbor atom whose lattice site is along the  $C_3$  axial direction. The electron density at this atom is found to be 46%, among which the  $s$  density is 7% and  $p$  density is 39%. This is in good agreement with our EPR hyperfine results (49% total density and 4%  $s$  density). In contrast, the result for  $V_{\text{As}}^0$  shows a large  $s$  density (17%) at the atom and is hardly compatible with our EPR results. This once again favors this  $V_{\text{Ga}}^{2-}$  model for the measured EPR spectrum.

#### IV. DISCUSSION

The EPR observation of Ga vacancy reported in this work permits a further improved comprehension about the native defects in GaAs.

(i) To correlate with DLTS results on electron-irradiated  $p$ -type GaAs, we note that six hole traps (labeled  $H0$ – $H5$ ) have been detected. The production rate of  $0.03 \text{ cm}^{-1}$  determined for our new EPR center is comparable to those obtained for the  $H2$  ( $E_v + 0.42$  eV) and  $H4$  ( $E_v + 0.79$  eV) levels. Particular interest should be paid to the  $H2$  level because this level was also observed in proton-irradiated GaAs where it was found to anneal at about 280 K.<sup>25</sup> The exact level position of our EPR center could not be determined from EPR measurements under optical excitation for photon energies of 0.5–1.4 eV, no light-induced change of the spectrum could be

detected. Additionally, another spectrum<sup>5</sup> of large intensity emerges under the light in the same field range as the new spectrum.

(ii) A defect-removal stage at room temperature in electron-irradiated GaAs has been observed in other experimental studies. From electrical resistivity measurements, Thommen<sup>26</sup> first found the thermal-annealing stages centered at about 235 and 280 K in  $n$ -type GaAs samples irradiated at low temperatures. Hall-effect measurements<sup>27,28</sup> confirmed the removal of irradiation-induced defects in  $n$ -type GaAs at 250 K. DLTS studies discovered two electron traps in  $n$ -type GaAs which can anneal below room temperature, but their production rates are quite low ( $10^{-3} \text{ cm}^{-1}$ ).<sup>2</sup> For  $p$ -type GaAs, recent PA studies of vacancy defects in electron-irradiated material<sup>11</sup> showed a principal annealing stage at about 300–340 K; the defect has been attributed to a  $V_{\text{Ga}}$ -related defect. This identification supports our present EPR observation.

(iii) From Fig. 5, it can be seen that the thermal stability of Ga vacancy depends on the dose of irradiation: the higher the electron dose is, the more evident the annealing effect becomes. This demonstrates that the annealing is Fermi-level dependent. It should be also noted that the annealing is not complete at room temperature, i.e., a partial annealing. In the sample of the largest dose ( $1 \times 10^{18} \text{ cm}^{-2}$ ), the Ga-vacancy concentration was first found to be reduced by a factor of about 2 and then no more annealing reduction was detected.

#### V. SUMMARY

We report the observation of an EPR spectrum in electron-irradiated Zn-doped  $p$ -type GaAs. This spectrum together with the  $\text{As}_{\text{Ga}}$  spectrum are the dominant EPR spectra detected under thermal equilibrium conditions at 4 K. From both the experimental observation and the TBGF calculation we identify this defect as a trigonal distorted Ga vacancy in the 2– charge state.

#### ACKNOWLEDGMENTS

One of us (Y.Q.J.), being on leave from the Department of Physics of the Peking University, wishes to acknowledge the financial support from the State Education Committee of China and the French Ministry of Foreign Office and the kind reception by Groupe de Physique des Solides, Université Paris 7 during this work. Group de Physique des Solides is "Unité Associée au Centre National de la Recherche Scientifique."

<sup>1</sup>For a recent review, see J. C. Bourgoin, H. J. von Bardeleben, and D. Stievenard, *J. Appl. Phys.* **64**, R65 (1988).

<sup>2</sup>D. Pons and J. C. Bourgoin, *J. Phys. C* **18**, 3839 (1985).

<sup>3</sup>D. Stievenard, X. Boddart, and J. C. Bourgoin, *Phys. Rev. B* **34**, 4048 (1986).

<sup>4</sup>C. Corbel, M. Stucky, P. Hautajarvi, K. Saarinen, and P. Moser, *Phys. Rev. B* **38**, 8192 (1988).

<sup>5</sup>H. J. von Bardeleben and J. C. Bourgoin, *Phys. Rev. B* **33**, 2890 (1986).

<sup>6</sup>H. J. von Bardeleben, J. C. Bourgoin, and A. Miret, *Phys. Rev. B* **34**, 1360 (1986).

<sup>7</sup>J. Maguire, R. Murray, R. C. Newman, R. B. Beall, and J. J. Harris, *Appl. Phys. Lett.* **50**, 516 (1987).

<sup>8</sup>D. G. Deppe, N. Holonyak, Jr., W. E. Plano, V. M. Robbins,

- J. M. Dallessasse, K. C. Hsieh, and I. E. Baker, *J. Appl. Phys.* **64**, 1838 (1988).
- <sup>9</sup>G. Baraff and M. Schlüter, *Phys. Rev. Lett.* **55**, 1327 (1985).
- <sup>10</sup>D. V. Lang, R. A. Logan, and L. C. Kimerling, *Phys. Rev. B* **15**, 4874 (1977).
- <sup>11</sup>F. Pierre, Ph.D. thesis, Université Paris XI, 1989.
- <sup>12</sup>The As-antisite spectrum in our samples has been studied to compare with that in electron-irradiated *n*-type and semi-insulating GaAs samples. More results are planned to be reported in another paper.
- <sup>13</sup>T. A. Kennedy and M. G. Spencer, *Phys. Rev. Lett.* **57**, 2690 (1986).
- <sup>14</sup>The spin-electron localization can be estimated through comparing the measured hyperfine interactions with the corresponding values of the free atom, taken from J. R. Morton and K. F. Preston, *J. Magn. Res.* **30**, 577 (1978).
- <sup>15</sup>U. Kaufmann, M. Baeumler, J. Windscheif, and W. Wilkening, *Appl. Phys. Lett.* **49**, 1254 (1986).
- <sup>16</sup>K. Krambrock, B. K. Meyer, and J. M. Spaeth, *Phys. Rev. B* **39**, 1973 (1989).
- <sup>17</sup>E. Christoffel, T. Benchiguer, A. Goltzene, C. Schwab, G. Wang, and J. Wu, *Phys. Rev. B* **42**, 3461 (1990).
- <sup>18</sup>We have used a self-consistent TBGF formalism which has been applied to many cases. See, for example, C. Delerue, M. Lannoo, and G. Allan, *Phys. Rev. B* **39**, 1669 (1989). The band structure of the perfect crystal is calculated with the empirical parameters given in D. N. Talwar and C. S. Ting, *ibid.* **25**, 2660 (1982).
- <sup>19</sup>C. Delerue (unpublished).
- <sup>20</sup>H. Xu and U. Lindefelt, *Phys. Rev. B* **41**, 5979 (1990).
- <sup>21</sup>J. van der Rest and P. Pêcheur, *J. Phys. C* **17**, 85 (1984).
- <sup>22</sup>P. J. Lin-Chung and T. L. Reinecke, *Phys. Rev. B* **27**, 1101 (1983).
- <sup>23</sup>G. D. Watkins, *Phys. Rev. Lett.* **33**, 223 (1974).
- <sup>24</sup>M. Lannoo, *Phys. Rev. B* **36**, 9355 (1987).
- <sup>25</sup>W. O. Siyanbola and D. W. Palmer, *Phys. Rev. Lett.* **66**, 56 (1991).
- <sup>26</sup>K. Thommen, *Radiat. Eff.* **2**, 201 (1970).
- <sup>27</sup>H. J. Stein, *J. Appl. Phys.* **40**, 5300 (1969).
- <sup>28</sup>M. U. Jeong, J. Shirafuji, and Y. Inuishi, *Radiat. Eff.* **10**, 93 (1971).